Time-dependent change of in vivo optical imaging of oxidative stress in the mouse stroke model

Yumiko Nakano, Toru Yamashita, Qian Li, Kota Sato, Yasuyuki Ohta, Ryuta Morihara, Nozomi Hishikawa, and Koji Abe*

Department of Neurology, Okayama University Graduate School of Medicine, Dentistry and Pharmaceutical Sciences, Okayama, Japan

***Corresponding author:** Koji Abe, Department of Neurology, Okayama University Graduate School of Medicine, Dentistry and Pharmaceutical Sciences, 2-5-1 Shikata-cho, Kita-ku, Okayama 700-8558, Japan

Tel: +81-86-235-7365; fax: +81-86-235-7368; email: tuberose0902ny@gmail.com

Running head: In vivo imaging of oxidative stress after tMCAO

Name of Associate Editor: Hideyuki Okano, PhD

Key words: in vivo imaging; ischemia-reperfusion injury; Nrf2; OKD mouse; oxidative stress; stroke; Resource Identification Initiative.

Support or grant information: This work was partly supported by Grants-in-Aid for Scientific Research (B, 25293202), (C, 15K09316) and Challenging Research (15K15527) and Young Research (15K21181), and by Grants-in-Aid from the Research Committees (Mizusawa H, Nakashima K, Nishizawa M, Sasaki H, and Aoki M) from the Ministry of Health, Labour and Welfare of Japan.

ABSTRACT

Nuclear factor erythroid 2-related factor 2 (Nrf2) plays a pivotal role in cellular defense against oxidative stress damage after ischemic stroke. In the present study, we examined the time-dependent change of in vivo optical imaging of oxidative stress after stroke with Keap1-dependent oxidative stress detector (OKD) mice. OKD mice were subjected to transient middle cerebral artery occlusion (tMCAO) for 45 min, and in vivo optical signals were detected during the pre-operative period, 12 h, 1 d, 3 d, and 7 d after tMCAO. Ex vivo imaging was performed immediately after obtaining in vivo optical signals at 1 d after tMCAO. Immunohistochemical analyses and infarct volume were also examined after in vivo imaging at each period. The in vivo signals showed a peak at 1 d after tMCAO that was slightly correlated to infarct volume. The strong ex vivo signals, which were detected in the peri-ischemic area, corresponded to endogenous Nrf2 expression. Moreover, endogenous Nrf2 expression was detected mainly in neurons followed by oligodendrocytes and pericytes, but only slightly in astrocytes, microglia, endothelial cells. The present study successfully demonstrated the temporal change of in vivo imaging of oxidative stress after tMCAO, which is consistent with strong expression of endogenous Nrf2 in the peri-ischemic area with a similar time course.

SIGNIFICANCE

This study investigated the time-dependent change of in vivo optical imaging of oxidative stress after stroke with OKD mice. The in vivo signals showed a peak at 1 d after tMCAO that was slightly correlated to infarct volume. The strong ex vivo signals, which were detected in the peri-ischemic area, corresponded to endogenous Nrf2 expression. Our result of synchronization between in vivo imaging and endogenous Nrf2 expression might provide a benefit to verification of drugs targeting the Nrf2-mediated defense pathway and the therapeutic time window in acute phase of ischemic stroke.

INTRODUCTION

Although early recanalization of the ischemic brain is essential to rescue the peri-ischemic area surrounding the ischemic core and to restore neurological functions, such recanalization may also result in tissue damage known as “reperfusion injury” (Abe et al. 1988; Molina and Alvarez-Sabin 2009). Reactive oxygen species (ROS), which begin to be produced during cerebral ischemia, are then exaggerated during reperfusion (Chan 1996; Chan 2001; Peters et al. 1998), triggering oxidative damage to DNA, lipids, and proteins, finally resulting in cell death (Jung et al. 2010; Lakhan et al. 2009). Therefore, detection and regulation of ROS is indispensable in ischemia-reperfusion injury.

Nuclear factor erythroid 2-related factor 2 (Nrf2) is a redox-sensitive transcription factor that regulates the cellular defense enzymes against oxidative stress. Under quiescent conditions, Nrf2 is combined with kelch-like ECH associating protein 1 (Keap1) which promotes rapid proteasomal degradation of Nrf2 via ubiquitination. However, under oxidative stress conditions, the dissociation of Keap1 frees Nrf2 from ubiquitin/proteasome degradation, and Nrf2 binds to the antioxidant response element (ARE) that leads to the induction of phase II defense enzyme expression (Ishii et al. 2000; Kaspar et al. 2009; Kensler et al. 2007; Shih et al. 2005).

Recent studies suggested that Nrf2 is induced after cerebral ischemia, especially in the peri-ischemic area of the animal stroke model (Alfieri et al. 2011; Dang et al. 2012; Takagi et al. 2014; Takamiya et al. 2012). However, each report shows a different temporal change in Nrf2 expression after cerebral ischemia. Furthermore, the time-dependent change of such anti-oxidative stress response in cerebral ischemia in vivo has not been fully investigated. On the other hand, there are several studies that have focused on in vivo imaging analysis of the acute response to ischemia-reperfusion injury such as autophagy, inflammation, and early stage apoptosis (Liu et al. 2010; Martin et al. 2015; Medoc et al. 2016; Takamiya et al. 2012; Tian et al. 2010). In the present study, therefore, we examined the time-dependent change of in vivo optical imaging of oxidative stress after cerebral ischemia using a Keap1-dependent oxidative stress detector, No.48 (OKD48) transgenic mouse which is able to visualize oxidative stress (Oikawa et al. 2012), and concurrently validated the temporal change in Nrf2 and related protein expression in immunohistochemical analysis.

METHODS AND MATERIALS

Animals

We obtained OKD48 transgenic mice from TransGenic Inc. (Japan) and

maintained this line as heterozygotes by screening offspring by genotyping using the polymerase chain reaction (PCR). The OKD48 construct consists of three copies of AREs as an optimized stress-inducible promoter, Nrf2, and FLAG-tagged luciferase (Oikawa et al. 2012). Under quiescent conditions, this transgene is not transcriptionally induced and the leaked fusion protein is degraded by Keap1. However, under oxidative stress conditions, the transgene is induced by endogenous Nrf2 dissociated from Keap1, and the fusion protein enables oxidative stress to be visualized as bioluminescence when luciferin is injected.

Age and gender-matched groups of male and female mice (11-13 weeks old, 23-28 g, total n = 32) were used in each experimental group. All mice were allowed free access to water and food in a temperature-regulated room (23-25°C) and placed in a 12 h light-dark cycle. All experimental procedures were carried out according to the guidelines of the Animal Care and Committee of the Graduate School of Medicine, Dentistry, and Pharmaceutical Sciences, Okayama University (approval #OKU-2014536).

To detect an increase of bioluminescent signals at 12 h after surgery inducing cerebral ischemia in comparison to pre-operative period with a two-sided 5% significance level and a power of 80%, a sample size of 6 mice was necessary. We used

48 mice in this study, of which 16 were excluded based on the following exclusion criteria: mice that died as a result of a procedural problem during surgery (n = 3), mice without neurological findings or in vivo optical signals (n = 6), and mice that died after surgery in the period leading up to sacrifice (n = 7). Finally, we included 5-8 mice in each group based on time course, in addition to 2 mice for ex vivo imaging. Because ex vivo imaging was examined for identification of a bioluminescent signal distribution, we performed ex vivo imaging in 2 mice as the representatives. The experimenter who conducted operations and in vivo / ex vivo optical imaging was not blinded to the assignment of animals to each group depending on observation period because this study is not interventional, but observational. However, in immunohistochemical analyses, the estimator was blinded to each mice brain section for the validity.

Focal cerebral ischemia

Focal cerebral ischemia was introduced into mice by transient middle cerebral artery occlusion (tMCAO) according to our previous reports (Abe et al. 1992; Yamashita et al. 2006). Briefly, mice were anesthetized with a nitrous oxide: oxygen: isoflurane mixture (69%: 30%: 1%) through an inhalation mask. The right common carotid artery was exposed and a 7-0 nylon thread with a silicone-coated tip was

inserted into the right MCA while body temperature was maintained at 37 ± 0.3°C using a heat bed (BWT-100; Bio Research Center, Japan). After 45 min of tMCAO, the silicone-coated thread was pulled out to restore blood flow (reperfusion). Then, the incision was closed, and the animals recovered and were allowed free access to water and food at ambient temperature. Sham control animals (n = 4) were prepared with a sham cervical operation but without inserting the thread.

In vivo and ex vivo optical imaging of oxidative stress

Bioluminescent imaging was performed in each group of OKD48 mice using the IVIS spectrum imaging system (PerkinElmer Inc., USA). During the pre-operative period, 12 h, 1 d, 3 d, and 7 d after tMCAO (each n = 5-8), mice were intraperitoneally injected with 150 mg/kg of D-luciferin (OZ Biosciences, USA) dissolved in phosphate-buffered saline (PBS) 20 min before in vivo optical imaging for 1 min exposure under constant anesthesia, as indicated above. The in vivo signals were detected on a skull surface with a head skin opened. Every time after performing in vivo imaging, the head skin was sutured and completely closed to prevent excessive bleeding, damage due to drying, or infection. A part of mice brains at 1 d (n = 2) was quickly removed after in vivo imaging, and was cut into 2 mm thick sections, then ex vivo

imaging was performed under the same conditions as in vivo. Bioluminescent signals were measured from the skull surface using uniform circular regions of interest (ROIs), and emission intensity was expressed as the total flux of photons (photons/sec) by LivingImage software (PerkinElmer).

Tissue preparation and measurement of infarct volume

After obtaining in vivo optical signals, sham-operated mice (n=4) and stroke mice (n = 6 at 12 h, n = 5 at 1 d, n = 6 at 3 d, and n = 8 at 7 d after tMCAO) were deeply anesthetized by intraperitoneal injection of pentobarbital (40 mg/kg), and then perfused with chilled PBS, followed by 4% paraformaldehyde in PBS. Brains were removed and immersed in the same fixative solution overnight, then were subsequently incubated in 20% (wt/vol) sucrose in PBS for 24 h at 4°C. The tissues were frozen in liquid nitrogen and stored at -80°C. Coronal brain sections 20 μm thick were prepared using a cryostat at -20°C and mounted on silane-coated glass slides.

These brain sections were stained with cresyl violet as Nissle staining to measure the infarct area using a standard computer-assisted image analysis technique. The infarct volume of each brain was calculated by summation of infarct areas of five serial brain slices, at a 0.5 mm interval each, between 1.0 mm anterior and 1.5 mm

posterior to the bregma.

Immunohistochemistry

For immunohistochemistry, frozen sections (20 μm) were incubated in 0.3% hydrogen peroxide/methanol for 20 min to prevent endogenous peroxidase activity. After washing in PBS, brain sections were blocked in 5% bovine serum albumin for 2 h. Then, they were incubated 4°C overnight with the following primary antibodies. All antibodies used in this study were from commercial sources (see Table 1): rabbit anti-Nrf2 antibody (1:200; Sigma-Aldrich, USA, SAB4501984, AB_10747179); mouse anti-luciferase antibody (1:100; Sigma, L2164, AB_439707); goat anti-Keap1 antibody (1:50; Santa Cruz Biotechnology, USA, sc-15246, AB_2132638); rabbit anti-HO-1 antibody (1:500; Stressgen, Canada, SPA-895, AB_2314637). The sections were washed in PBS and incubated with biotinylated secondary antibodies (Vector Laboratories, USA) diluted at 1:500 for 2.5 h. The sections were then incubated with the ABC Elite complex (Vector Laboratories), and visualized with diaminobenzidine (DAB) substrate dissolved in PBS. A set of sections was also stained in a similar way but without the primary antibody and served as the negative control.

For double immunofluorescent staining, frozen sections (20 μm) were blocked

in Tris-NaCl-blocking (TNB) buffer (PerkinElmer). The primary antibodies used were: rabbit anti-Nrf2 antibody (1:100; Sigma, SAB4501984, AB_10747179); mouse anti-luciferase antibody (1:50; Sigma, L2164, AB_439707); mouse anti-NeuN antibody for neuron (1:200; Millipore, Germany, MAB377, AB_2298772); mouse anti-GFAP antibody for astrocytes (1:500; Millipore, MAB3402, AB_10627989); goat anti-Iba1 antibody for microglia (1:200, Abcam, UK, ab107159, AB_10972670); goat anti-GSTπ antibody for oligodendrocytes (1:200; Abcam, ab53943, AB_873819); lycopersicon esculentum (LEL) for vascular endothelial cells (1:200; Vector Laboratories, DL-1174, AB_2336404); mouse anti-NG2 antibody for pericytes (1:500; Millipore, 05-710, AB_309925). Biotinylated anti-rabbit secondary antibody (1:500, Vector Laboratories) was used to estimate Nrf2 expression. Other immunogens were detected with secondary antibodies conjugated with Alexa Fluor™ (1:500; Invitrogen, USA). The sections were finally treated with a tyramide signal amplification kit (TSA tetramethyl rhodamine system; PerkinElmer) to detect Nrf2 immunoreactivity.

Semiquantitative analysis

For the semiquantitative evaluation of histochemical staining, three areas were randomly selected from the sections at the level of striatum, and captured at 200×

magnification with a light microscope (OlympusBX51, Olympus, Japan). The number of positively stained cells in each field was counted, and the same procedure was repeated for each section. We confirmed the border between the infarcted and peri-ischemic region through Nissle staining of adjacent sections based on a previous report (Omori et al. 2002).

Statistical analysis

Data were analyzed in SPSS v.22.0 (IBM, USA, SCR_002865). All data are expressed as mean ± SE or median [interquartile range]. Based on normality tests of data, unpaired t-test and Mann-Whitney U test were performed to examine the differences between sexes in infarct volume and bioluminescent signals, respectively. The differences in bioluminescent signals between the preoperative period and each time point after tMCAO were evaluated with Wilcoxon signed-rank test. The correlation between infarct volume and peak bioluminescent signals was evaluated using Kendall rank correlation coefficient. One-way ANOVA was used to verify the differences in the expression of Nrf2, luciferase, Keap1, and HO-1 among each period, followed by a Turkey's honestly significant difference test. The differences between peri-ischemic area and ischemic core were evaluated with paired t-test. In all statistical analyses,

significance was accepted at $p < 0.05$.

RESULTS

There were no differences both in infarct volume and bioluminescent signals between the sexes (infarct volume: males = 8.7 ± 4.1 mm^3; females = 9.7 ± 6.7 mm^3; n = 15 and 11, respectively; $p > 0.05$, unpaired t-test; in vivo peak signals: males = 3.2 [1.3-4.2] $\times 10^6$ photons/sec; females = 2.0 [1.2-2.8] $\times 10^6$ photons/sec; n = 15 and 11, respectively; $p > 0.05$, Mann-Whitney U test). Fig. 1A shows a typical time-dependent change of in vivo bioluminescent signals indicative of oxidative stress before and after tMCAO in the same mouse. The signals, which became detectable from 12 h after tMCAO, peaked at 1 d (pre = 2.7 [2.4-2.9] $\times 10^6$ photons/sec; 1 d = 4.0 [3.1-9.3] $\times 10^6$ photons/sec; n = 8; $^{**}p < 0.01$, Wilcoxon signed-rank test), decreased until 3 d, then finally disappeared at 7 d. The in vivo peak signals at 1 d after tMCAO were slightly correlated with infarct volume (R = 0.333, $p = 0.072$, Kendall rank correlation coefficient, Fig. 1B). Ex vivo imaging of coronal brain slices at 1 d after tMCAO showed high bioluminescent signals in the marginal area of MCA territory surrounding the ischemic core which was unstained in Nissle staining (Fig. 1C, D).

Immunohistochemical analysis showed no evident Nrf2 staining in sham

control brains, but was apparent in the peri-ischemic area of mice brains with tMCAO. The number of Nrf2-positive cells peaked at 12 h in the peri-ischemic area, then gradually decreased until 7 d ($F_{4, 25}$ = 13.0; n = 30; $p < 0.01$, one-way ANOVA; sham control [n = 4] vs 12 h [n = 7], 1 d [n = 5], 3 d [n = 6], and 7 d [n = 8]; *$p < 0.05$, **$p < 0.01$, Turkey's honestly significant difference test; Fig. 2, left upper panel), and was always higher than the ischemic core (n = 5-8; $^{\#\#}p < 0.01$, paired t-test; Fig. 2, left upper panel). On the other hand, the expression of luciferase indicative of exogenous Nrf2 began to increase from 12 h, which peaked at 1 - 3 d, and then decreased at 7 d after tMCAO in the peri-ischemic area ($F_{4, 25}$ = 13.1; n = 30; $p < 0.01$, one-way ANOVA; sham control [n = 4] vs 12 h [n = 7], 1 d [n = 5], 3 d [n = 6], and 7 d [n = 8]; **$p < 0.01$, Turkey's honestly significant difference test; Fig. 2, right upper panel). Those luciferase expressions were also stronger in the peri-ischemic area than the ischemic core (n = 5-8; $^{\#}p < 0.05$, $^{\#\#}p < 0.01$, paired t-test; Fig. 2, right upper panel). A weak baseline expression level of Keap1 was observed in sham control brains, but declined at 12 h after tMCAO, and finally recovered at 7 d (not significant). Keap1-positive cells were variable in the peri-ischemic area (Fig. 2, left lower panel). The number of HO-1-positive cells began to increase from 12 h, peaked at 3 d in the peri-ischemic area, then decreased 7 d after tMCAO ($F_{4, 25}$ = 3.6; n = 30; $p < 0.05$, one-way ANOVA; sham control [n = 4] vs 12 h

[n = 7], 1 d [n = 5], 3 d [n = 6], and 7 d [n = 8]; *$p < 0.05$, **$p < 0.01$, Turkey's honestly significant difference test; Fig. 2, right lower panel), and was higher than the ischemic core (n = 5-8; $^{\#}p < 0.05$, $^{\#\#}p < 0.01$, paired t-test; Fig. 2, right lower panel).

Double immunofluorescent analysis showed that endogenous Nrf2 was detected both in the nucleus and cytoplasm with a peak at 12 h - 1 d (Fig. 3), while luciferase expression (exogenous Nrf2) was observed mainly in the cytoplasm, peaking at 1 - 3 d. Thus, Nrf2-luciferase double-positive cells were prominent at 1 d after tMCAO, followed by 3 d (Fig. 3, arrowheads). Cell-type specific analysis on Nrf2 expression profiles showed that Nrf2 immunofluorescent signals were apparently colocalized with NeuN presenting neurons, while a few merged signals were observed in the staining of Nrf2 with astrocytic GFAP, microglial Iba1, or endothelial LEL. On the other hand, several cells expressing Nrf2 were also positive for GSTπ of oligodendrocyte or NG2 of pericyte marker (Fig. 4, arrowheads).

DISCUSSION

The generation of ROS explosively increases under cerebral ischemia-reperfusion injury (Allen and Bayraktutan 2009; Chan 1996; Chan 2001; Peters et al. 1998), and is one of the pivotal mechanisms leading to ischemic cell death.

The Keap1-Nrf2 defense pathway plays a key role against such ROS-mediated oxidative stress in cerebral ischemia (Alfieri et al. 2011; Li et al. 2011; Shih et al. 2005; Takagi et al. 2014). In the present study, we showed the temporal change of in vivo optical imaging of oxidative stress caused by ischemia-reperfusion injury in OKD48 mouse stroke model with the peak signals at 1 d after tMCAO, which was consistent with a previous report (Takagi et al. 2014).

Takagi et al. evaluated Nrf2-mediated anti-oxidative stress response with GFP signals by using OKD mice whose construct contained GFP instead of luciferase (Takagi et al. 2014). They confirmed the distribution of GFP signals indicative of oxidative stress mainly in the peri-ischemic region, which corresponded to our results of ex vivo imaging. Another study reported autophagy imaging in an experimental mouse stroke brain, and ex vivo fluorescent signals indicative of autophagosomes were detected in the peri-ischemic area of the ischemic cortex (Tian et al. 2010). Thus, in recent years, various responses against ischemia-reperfusion injury such as oxidative stress (Takagi et al. 2014), autophagy (Tian et al. 2010), or pro-inflammatory (Takamiya et al. 2012) / pro-apoptotic (Liu et al. 2010) processes have been able to become visualized in vivo, particularly in the peri-ischemic region.

Bioluminescent signals are produced via the Keap1-Nrf2 pathway with the

luciferase assay. Consequently, we validated the time course of Nrf2 and other related protein expression by immunohistochemistry. Nrf2 expression was clearly detectable mainly in the peri-ischemic area at 12 h after tMCAO whereas in vivo peak signals were observed at 1 d after tMCAO. As described above, ROS converts the Keap1 structure to liberate and translocate Nrf2 into the nucleus, then the activated Nrf2 accelerates the expression of anti-oxidative stress proteins via ARE (Kaspar et al. 2009; Kobayashi and Yamamoto 2006; Motohashi and Yamamoto 2004). Previous studies reported an increase in Nrf2 expression at 4-48 h after cerebral ischemia (Li et al. 2011; Srivastava et al. 2013; Tanaka et al. 2011; Yang et al. 2009), as observed in our result. On the other hand, exogenous Nrf2-luciferase fusion protein is induced under continuously activated endogenous Nrf2 (Oikawa et al. 2012), which could delay the peak of in vivo exogenous Nrf2 optical signals after endogenous Nrf2 expression. Besides, an immunofluorescent luciferase signal was observed only in the cytoplasm because exogenous Nrf2-luciferase fusion protein has no DNA binding site (Oikawa et al. 2012).

In Nrf2 expression profiles based on cell type-specificity, previous studies indicated that Nrf2 is expressed mainly in neurons, and slightly in astrocytes or microglia (Dang et al. 2012; Shih et al. 2003; Takagi et al. 2014; Tanaka et al. 2011). Recently, another research showed Nrf2 expression in endothelial cells and pericytes

after ischemia-reperfusion injury in tMCAO model (Imai et al. 2016). Our present data was similar to these previous studies, but also found some Nrf2/GSTπ double-positive cells in the peri-ischemic area, suggesting that oligodendrocytes are more vulnerable to ischemic damage than other glial cells (Mifsud et al. 2014; Petito et al. 1998). In fact, multiple sclerosis showed nuclear Nrf2 expression in oligodendrocytes (Licht-Mayer et al. 2015). When we focused on the dimension of neurovascular unit (NVU) composed with neurons, glial cells, and vascular cells, our result indicated that Nrf2 was expressed in all components of NVU, especially in vulnerable cells such as neurons, oligodendrocytes, and pericytes, as a consequence of ischemia-reperfusion injury. Nrf2 activation may be beneficial for cell protection on NVU, particularly in the peri-ischemic region under oxidative stress after cerebral ischemia (Alfieri et al. 2011; Vargas and Johnson 2009).

In conclusion, we successfully demonstrated a temporal change of in vivo optical imaging of oxidative stress after ischemia-reperfusion injury, and found a slight correlation between the in vivo peak signals and infarct volume. Endogenous Nrf2 expression was observed in the peri-ischemic area, which corresponded to the ex vivo signal distribution. This endogenous Nrf2 was also detected mainly in neurons, and slightly in oligodendrocytes and pericytes, which were vulnerable to ischemic injury.

Our result of synchronization between in vivo imaging and endogenous Nrf2 expression might provide the benefit to verification of drugs targeting the Nrf2-mediated defense pathway and the therapeutic time window in acute phase of ischemic stroke in the future.

ACKNOWLEDGEMENTS

This work was partly supported by Grants-in-Aid for Scientific Research (B, 25293202), (C, 15K09316) and Challenging Research (15K15527) and Young Research (15K21181), and by Grants-in-Aid from the Research Committees (Mizusawa H, Nakashima K, Nishizawa M, Sasaki H, and Aoki M) from the Ministry of Health, Labour and Welfare of Japan.

COFLICT OF INTEREST

There is no conflict of interests to report.

ROLE OF AUTHORS

All authors had full access to all the data in the study and take responsibility for the integrity of the data and the accuracy of the data analysis. Study concept and design:

KA. Acquisition of data: YN, QL. Analysis and interpretation of data: YN, TY, KS, YO. Draft article for important intellectual content: YN, TY, KA. Statistical analysis: YN, RM, NH. Obtained funding: KA. Study supervision: KA.

REFERENCES

Abe K, Kawagoe J, Araki T, Aoki M, Kogure K. 1992. Differential expression of heat shock protein 70 gene between the cortex and caudate after transient focal cerebral ischaemia in rats. Neurol Res 14(5):381-385.

Abe K, Yuki S, Kogure K. 1988. Strong attenuation of ischemic and postischemic brain edema in rats by a novel free radical scavenger. Stroke 19(4):480-485.

Alfieri A, Srivastava S, Siow RC, Modo M, Fraser PA, Mann GE. 2011. Targeting the Nrf2-Keap1 antioxidant defence pathway for neurovascular protection in stroke. J Physiol 589(17):4125-4136.

Allen CL, Bayraktutan U. 2009. Oxidative stress and its role in the pathogenesis of ischaemic stroke. Int J Stroke 4(6):461-470.

Chan PH. 1996. Role of oxidants in ischemic brain damage. Stroke 27(6):1124-1129.

Chan PH. 2001. Reactive oxygen radicals in signaling and damage in the ischemic brain. J Cereb Blood Flow Metab 21(1):2-14.

Dang J, Brandenburg LO, Rosen C, Fragoulis A, Kipp M, Pufe T, Beyer C, Wruck CJ. 2012. Nrf2 expression by neurons, astroglia, and microglia in the cerebral cortical penumbra of ischemic rats. J Mol Neurosci 46(3):578-584.

Imai T, Takagi T, Kitashoji A, Yamauchi K, Shimazawa M, Hara H. 2016. Nrf2 activator

ameliorates hemorrhagic transformation in focal cerebral ischemia under warfarin anticoagulation. Neurobiology of disease 89:136-146.

Ishii T, Itoh K, Takahashi S, Sato H, Yanagawa T, Katoh Y, Bannai S, Yamamoto M. 2000. Transcription factor Nrf2 coordinately regulates a group of oxidative stress-inducible genes in macrophages. J Biol Chem 275(21):16023-16029.

Jung JE, Kim GS, Chen H, Maier CM, Narasimhan P, Song YS, Niizuma K, Katsu M, Okami N, Yoshioka H, Sakata H, Goeders CE, Chan PH. 2010. Reperfusion and neurovascular dysfunction in stroke: from basic mechanisms to potential strategies for neuroprotection. Mol Neurobiol 41(2-3):172-179.

Kaspar JW, Niture SK, Jaiswal AK. 2009. Nrf2:INrf2 (Keap1) signaling in oxidative stress. Free Radic Biol Med 47(9):1304-1309.

Kensler TW, Wakabayashi N, Biswal S. 2007. Cell survival responses to environmental stresses via the Keap1-Nrf2-ARE pathway. Annu Rev Pharmacol Toxicol 47:89-116.

Kobayashi M, Yamamoto M. 2006. Nrf2-Keap1 regulation of cellular defense mechanisms against electrophiles and reactive oxygen species. Adv Enzyme Regul 46:113-140.

Lakhan SE, Kirchgessner A, Hofer M. 2009. Inflammatory mechanisms in ischemic

stroke: therapeutic approaches. J Transl Med 7:97.

Li M, Zhang X, Cui L, Yang R, Wang L, Liu L, Du W. 2011. The neuroprotection of oxymatrine in cerebral ischemia/reperfusion is related to nuclear factor erythroid 2-related factor 2 (nrf2)-mediated antioxidant response: role of nrf2 and hemeoxygenase-1 expression. Biol Pharm Bull 34(5):595-601.

Licht-Mayer S, Wimmer I, Traffehn S, Metz I, Bruck W, Bauer J, Bradl M, Lassmann H. 2015. Cell type-specific Nrf2 expression in multiple sclerosis lesions. Acta Neuropathol 130(2):263-277.

Liu N, Deguchi K, Shang J, Zhang X, Tian F, Yamashita T, Ohta Y, Ikeda Y, Matsuura T, Abe K. 2010. In vivo optical imaging of early-stage apoptosis in mouse brain after transient cerebral ischemia. J Neurosci Res 88(16):3488-3497.

Martin A, Szczupak B, Gomez-Vallejo V, Domercq M, Cano A, Padro D, Munoz C, Higuchi M, Matute C, Llop J. 2015. In vivo PET imaging of the alpha4beta2 nicotinic acetylcholine receptor as a marker for brain inflammation after cerebral ischemia. J Neurosci 35(15):5998-6009.

Medoc M, Dhilly M, Matesic L, Toutain J, Krause-Heuer AM, Delamare J, Fraser BH, Touzani O, Barre L, Greguric I, Sobrio F. 2016. In Vivo Evaluation of Radiofluorinated Caspase-3/7 Inhibitors as Radiotracers for Apoptosis Imaging

and Comparison with [18F]ML-10 in a Stroke Model in the Rat. Mol Imaging Biol 18(1):117-126.

Mifsud G, Zammit C, Muscat R, Di Giovanni G, Valentino M. 2014. Oligodendrocyte pathophysiology and treatment strategies in cerebral ischemia. CNS Neurosci Ther 20(7):603-612.

Molina CA, Alvarez-Sabin J. 2009. Recanalization and reperfusion therapies for acute ischemic stroke. Cerebrovasc Dis 27 Suppl 1:162-167.

Motohashi H, Yamamoto M. 2004. Nrf2-Keap1 defines a physiologically important stress response mechanism. Trends Mol Med 10(11):549-557.

Oikawa D, Akai R, Tokuda M, Iwawaki T. 2012. A transgenic mouse model for monitoring oxidative stress. Sci Rep 2:229.

Omori N, Jin G, Li F, Zhang WR, Wang SJ, Hamakawa Y, Nagano I, Manabe Y, Shoji M, Abe K. 2002. Enhanced phosphorylation of PTEN in rat brain after transient middle cerebral artery occlusion. Brain Res 954(2):317-322.

Peters O, Back T, Lindauer U, Busch C, Megow D, Dreier J, Dirnagl U. 1998. Increased formation of reactive oxygen species after permanent and reversible middle cerebral artery occlusion in the rat. J Cereb Blood Flow Metab 18(2):196-205.

Petito CK, Olarte JP, Roberts B, Nowak TS, Jr., Pulsinelli WA. 1998. Selective glial

vulnerability following transient global ischemia in rat brain. J Neuropathol Exp Neurol 57(3):231-238.

Shih AY, Johnson DA, Wong G, Kraft AD, Jiang L, Erb H, Johnson JA, Murphy TH. 2003. Coordinate regulation of glutathione biosynthesis and release by Nrf2-expressing glia potently protects neurons from oxidative stress. J Neurosci 23(8):3394-3406.

Shih AY, Li P, Murphy TH. 2005. A small-molecule-inducible Nrf2-mediated antioxidant response provides effective prophylaxis against cerebral ischemia in vivo. J Neurosci 25(44):10321-10335.

Srivastava S, Alfieri A, Siow RC, Mann GE, Fraser PA. 2013. Temporal and spatial distribution of Nrf2 in rat brain following stroke: quantification of nuclear to cytoplasmic Nrf2 content using a novel immunohistochemical technique. J Physiol 591(14):3525-3538.

Takagi T, Kitashoji A, Iwawaki T, Tsuruma K, Shimazawa M, Yoshimura S, Iwama T, Hara H. 2014. Temporal activation of Nrf2 in the penumbra and Nrf2 activator-mediated neuroprotection in ischemia-reperfusion injury. Free Radic Biol Med 72:124-133.

Takamiya M, Miyamoto Y, Yamashita T, Deguchi K, Ohta Y, Abe K. 2012. Strong

neuroprotection with a novel platinum nanoparticle against ischemic stroke- and tissue plasminogen activator-related brain damages in mice. Neuroscience 221:47-55.

Tanaka N, Ikeda Y, Ohta Y, Deguchi K, Tian F, Shang J, Matsuura T, Abe K. 2011. Expression of Keap1-Nrf2 system and antioxidative proteins in mouse brain after transient middle cerebral artery occlusion. Brain Res 1370:246-253.

Tian F, Deguchi K, Yamashita T, Ohta Y, Morimoto N, Shang J, Zhang X, Liu N, Ikeda Y, Matsuura T, Abe K. 2010. In vivo imaging of autophagy in a mouse stroke model. Autophagy 6(8):1107-1114.

Vargas MR, Johnson JA. 2009. The Nrf2-ARE cytoprotective pathway in astrocytes. Expert Rev Mol Med 11:e17.

Yamashita T, Deguchi K, Sawamoto K, Okano H, Kamiya T, Abe K. 2006. Neuroprotection and neurosupplementation in ischaemic brain. Biochem Soc Trans 34(Pt 6):1310-1312.

Yang C, Zhang X, Fan H, Liu Y. 2009. Curcumin upregulates transcription factor Nrf2, HO-1 expression and protects rat brains against focal ischemia. Brain Res 1282:133-141.

FIGURE LEGENDS

Fig. 1) In vivo and ex vivo optical imaging of oxidative stress. (A) The time-dependent change of in vivo imaging during the pre-operative period and after tMCAO in the same mouse, showing a peak at 1 d (pre = 2.7 [2.4-2.9] $\times 10^6$ photons/sec; 1 d = 4.0 [3.1-9.3] $\times 10^6$ photons/sec; n = 8; $^{**}p < 0.01$, Wilcoxon signed-rank test). (B) A slight correlation between infarct volume and the in vivo peak signals at 1 d after tMCAO (R = 0.333, p = 0.072, Kendall rank correlation coefficient). (C) Ex vivo imaging of coronal brain slices at 1 d after tMCAO, showing strong signals in the peri-ischemic area. (D) Nissle staining of brain slices at 1 d after tMCAO. Unstained area surrounded by dotted line indicates ischemic core.

Fig. 2) Representative immunostaining of Nrf2, luciferase, Keap1, and HO-1 at 12 h, 1 d, 3 d, and 7 d after tMCAO in the peri-ischemic area (top panels), and semiquantitative analysis of the number of positive cells (/mm^2) (bottom panels). The number of Nrf2 positive cells peaked at 12 h after tMCAO in the peri-ischemic area, then decreased until 7 d (sham control [n = 4] vs 12 h [n = 7], 1 d [n = 5], 3 d [n = 6], and 7 d [n = 8]; $^{*}p < 0.05$, $^{**}p < 0.01$, Turkey's honestly significant difference test). The number of luciferase positive cells peaked at 1 - 3 d after tMCAO in the peri-ischemic area, and

then decreased at 7 d (sham control [n = 4] vs 12 h [n = 7], 1 d [n = 5], 3 d [n = 6], and 7 d [n = 8]; $^{**}p < 0.01$, Turkey's honestly significant difference test). A low baseline of Keap1 positive cells was slightly declined at 12 h after tMCAO, and recovered almost same level as sham control brains until 7 d (not significant). The number of HO-1-positive cells peaked at 3 d after tMCAO in the peri-ischemic area, then decreased at 7 d (sham control [n = 4] vs 12 h [n = 7], 1 d [n = 5], 3 d [n = 6], and 7 d [n = 8]; $^{*}p < 0.05$, $^{**}p < 0.01$, Turkey's honestly significant difference test). Those Nrf2-, luciferase-, Keap1-, and HO-1 expression levels in the peri-ischemic area were always higher than the ischemic core (n = 5-8; $^{\#}p < 0.05$, $^{\#\#}p < 0.01$, paired t-test).

Fig. 3) Double immunofluorescent analysis of Nrf2 and luciferase in the peri-ischemic area at 12 h, 1 d, 3 d, and 7 d after tMCAO. Arrowheads indicate Nrf2 and luciferase double-positive cells. Scale bar = 10 μm.

Fig. 4) Double immunofluorescent analysis of Nrf2 with cell type-specific markers for neurons (NeuN), astrocytes (GFAP), microglia (Iba1), and oligodendrocytes (GSTπ), endothelial cells (LEL), and pericytes (NG2) in the peri-ischemic area at 12 h after tMCAO. Arrowheads indicate double-positive cells for Nrf2 with each cell type-specific

marker. Scale bar = 10 μm.

Fig. 1

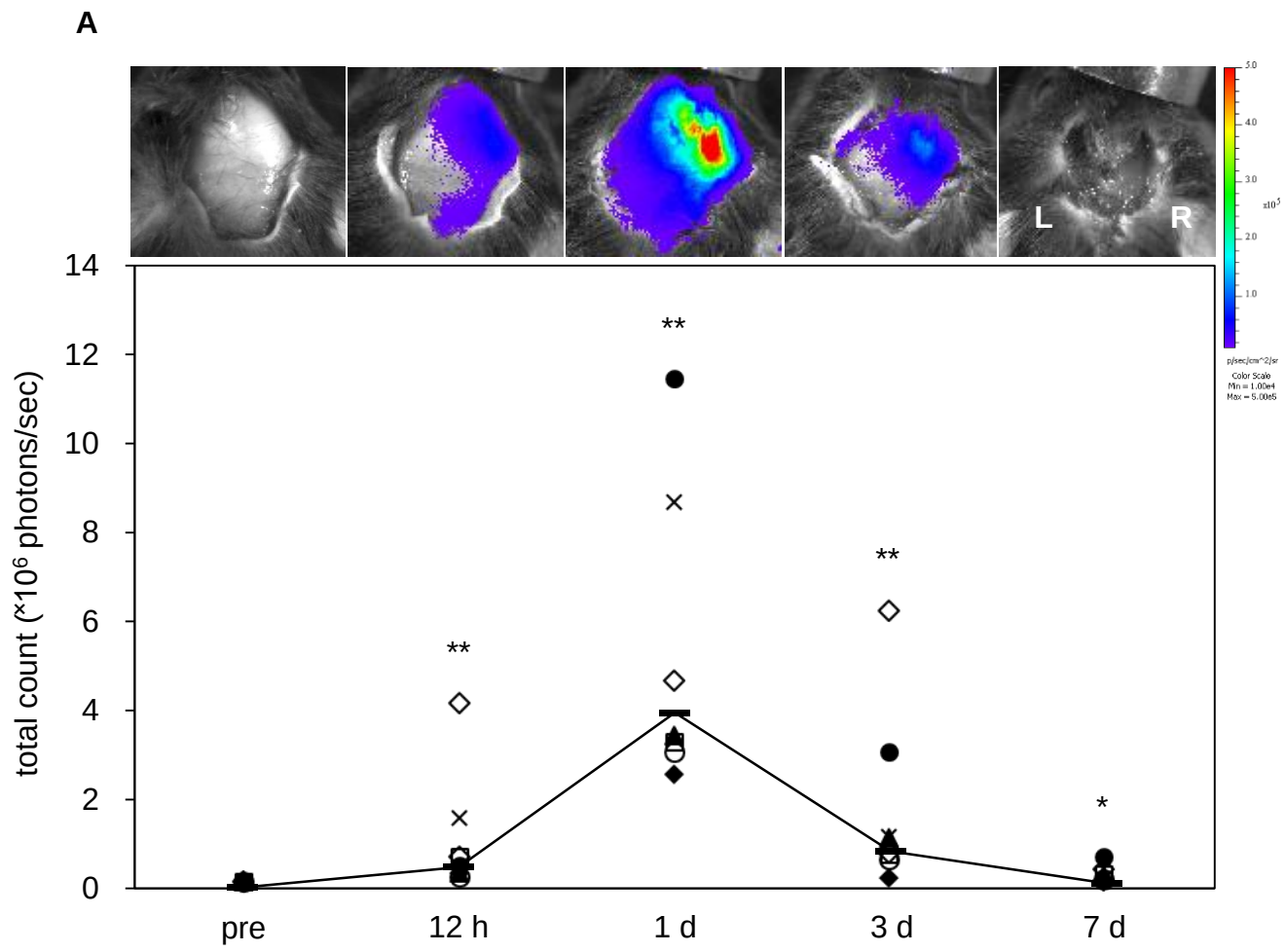
A
L
R
14
12
10
8
6
4
2
0
total count (×10⁶ photons/sec)
pre
12 h
1 d
3 d
7 d
**
**
**
*
p/sec/cm^2/sr
Color Scale
Min = 1.00e4
Max = 5.00e5

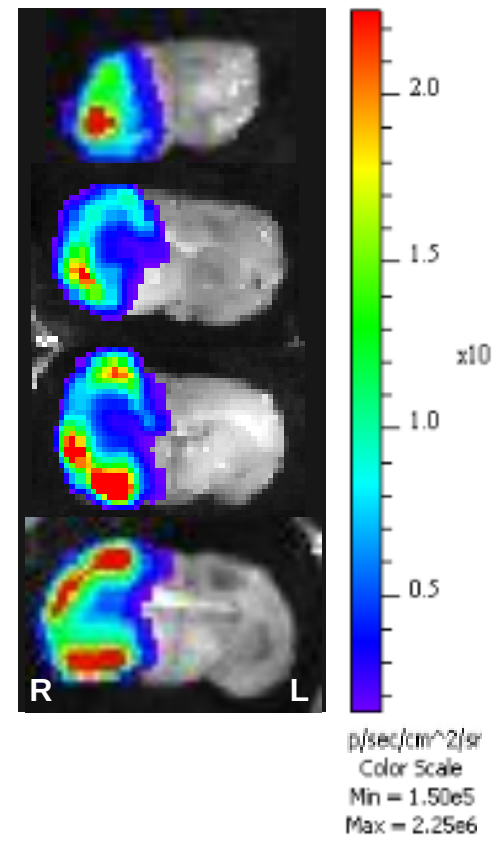
C
R
L
2.0
1.5
x10
1.0
0.5
p/sec/cm^2/sr
Color Scale
Min = 1.50e5
Max = 2.25e6

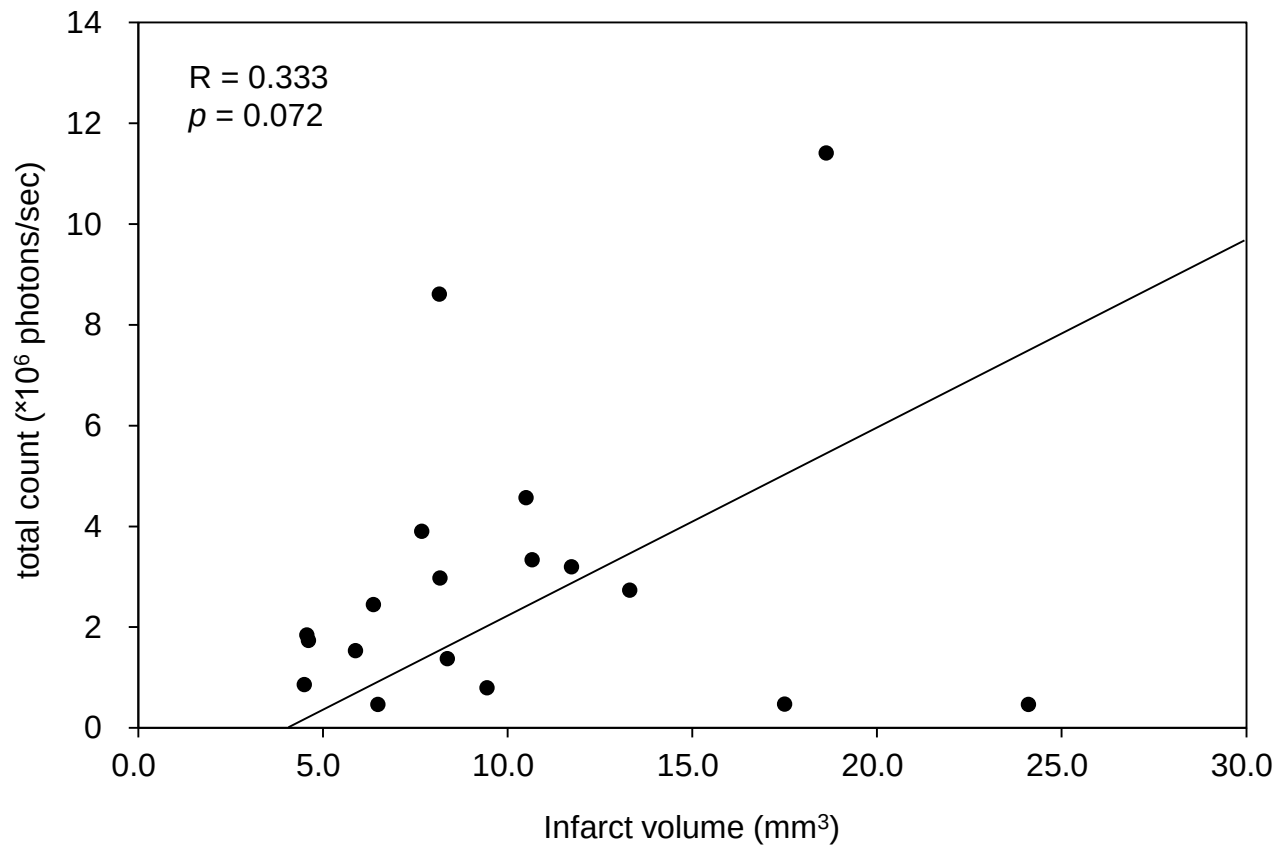
B
R = 0.333
p = 0.072
14
12
10
8
6
4
2
0
total count (×10⁶ photons/sec)
0.0
5.0
10.0
15.0
20.0
25.0
30.0
Infarct volume (mm³)

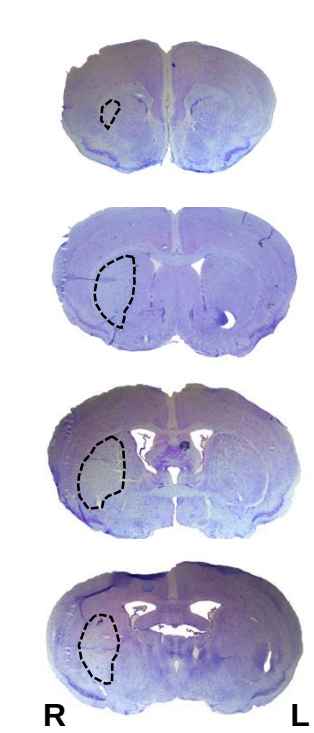
D
R
L

Fig. 2

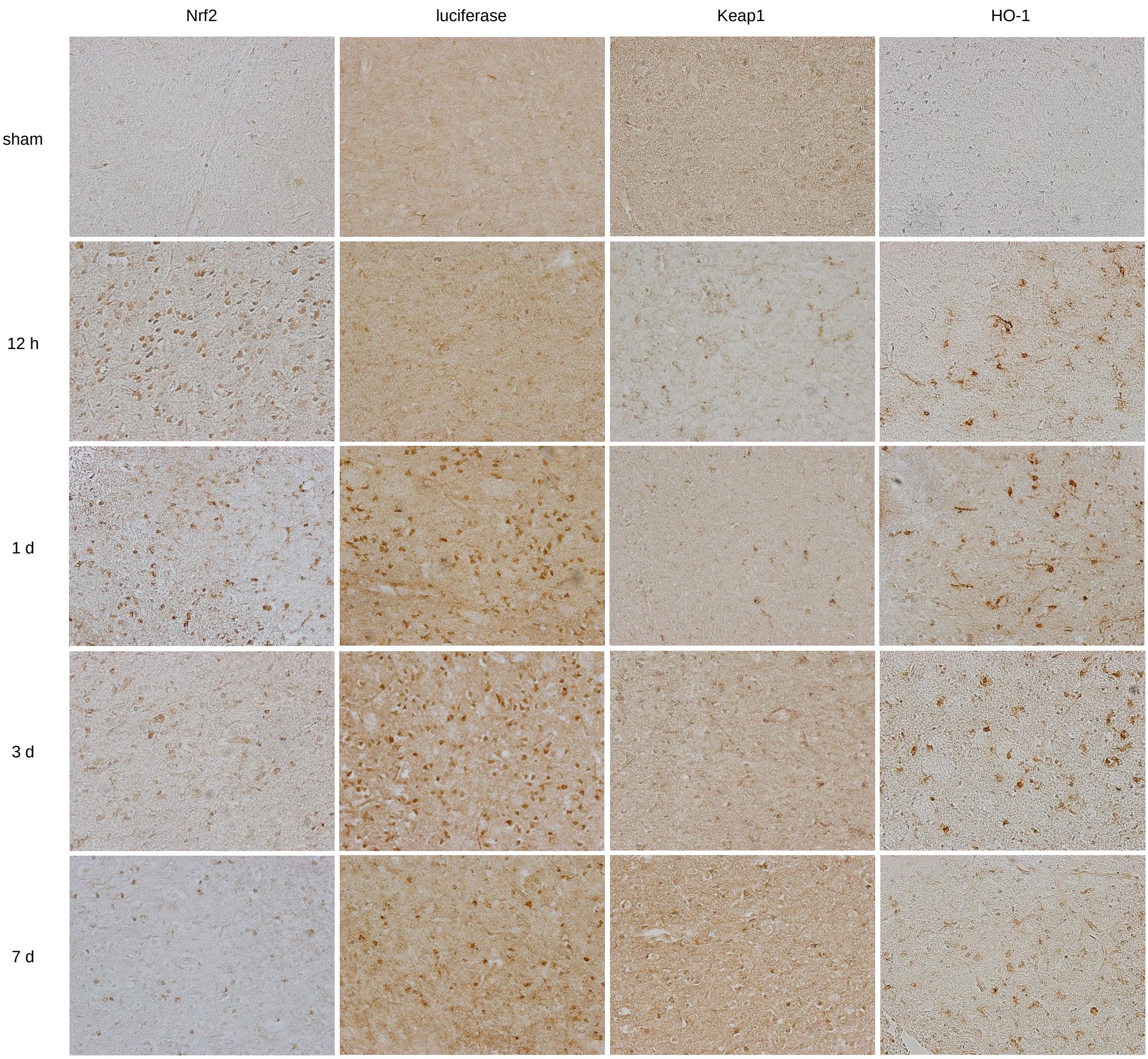
Nrf2
luciferase
Keap1
HO-1
sham
12 h
1 d
3 d
7 d

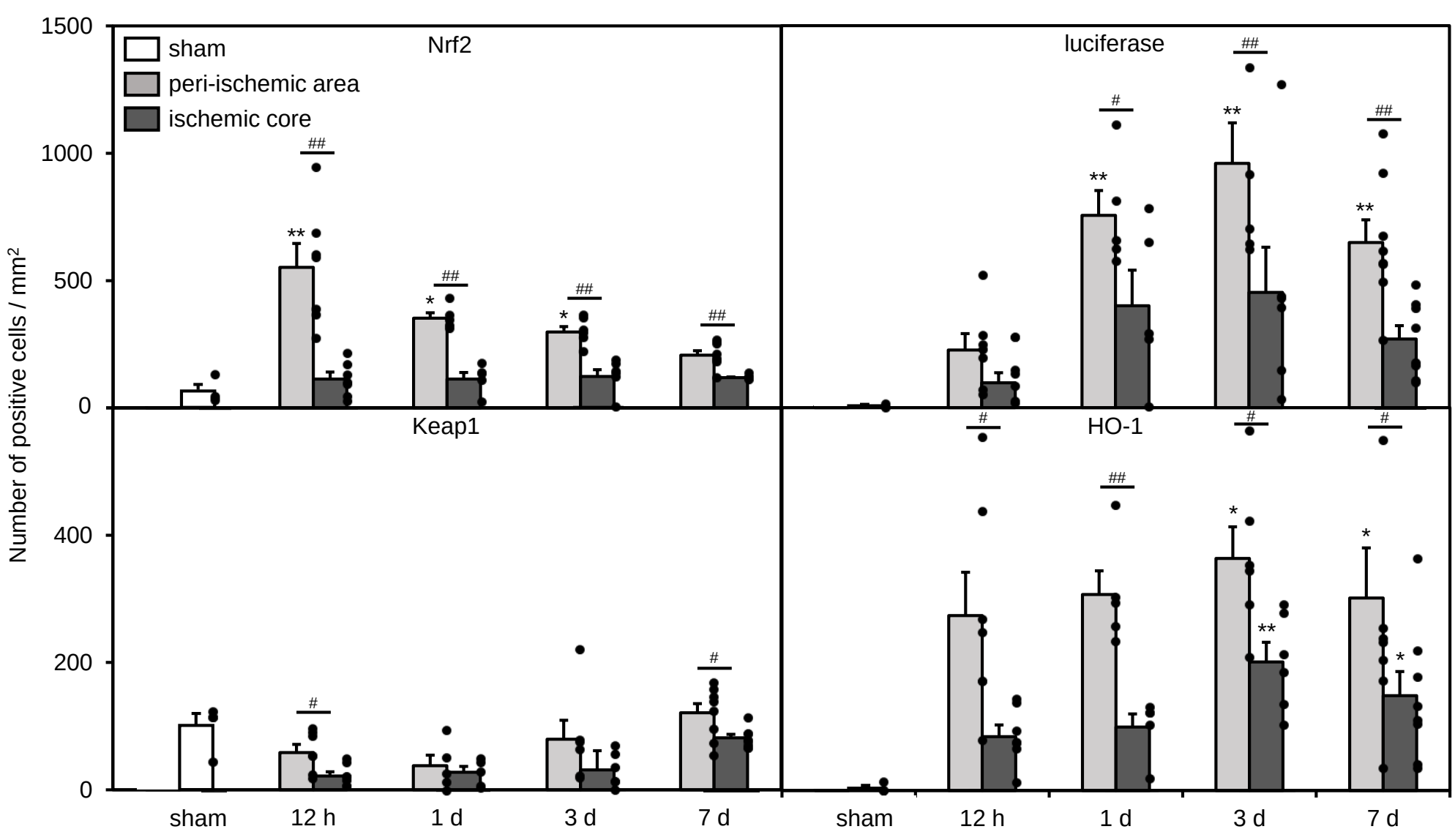
sham
peri-ischemic area
ischemic core
Nrf2
luciferase
Keap1
HO-1
Number of positive cells / mm²
1500
1000
500
0
400
200
sham
12 h
1 d
3 d
7 d

Fig. 3

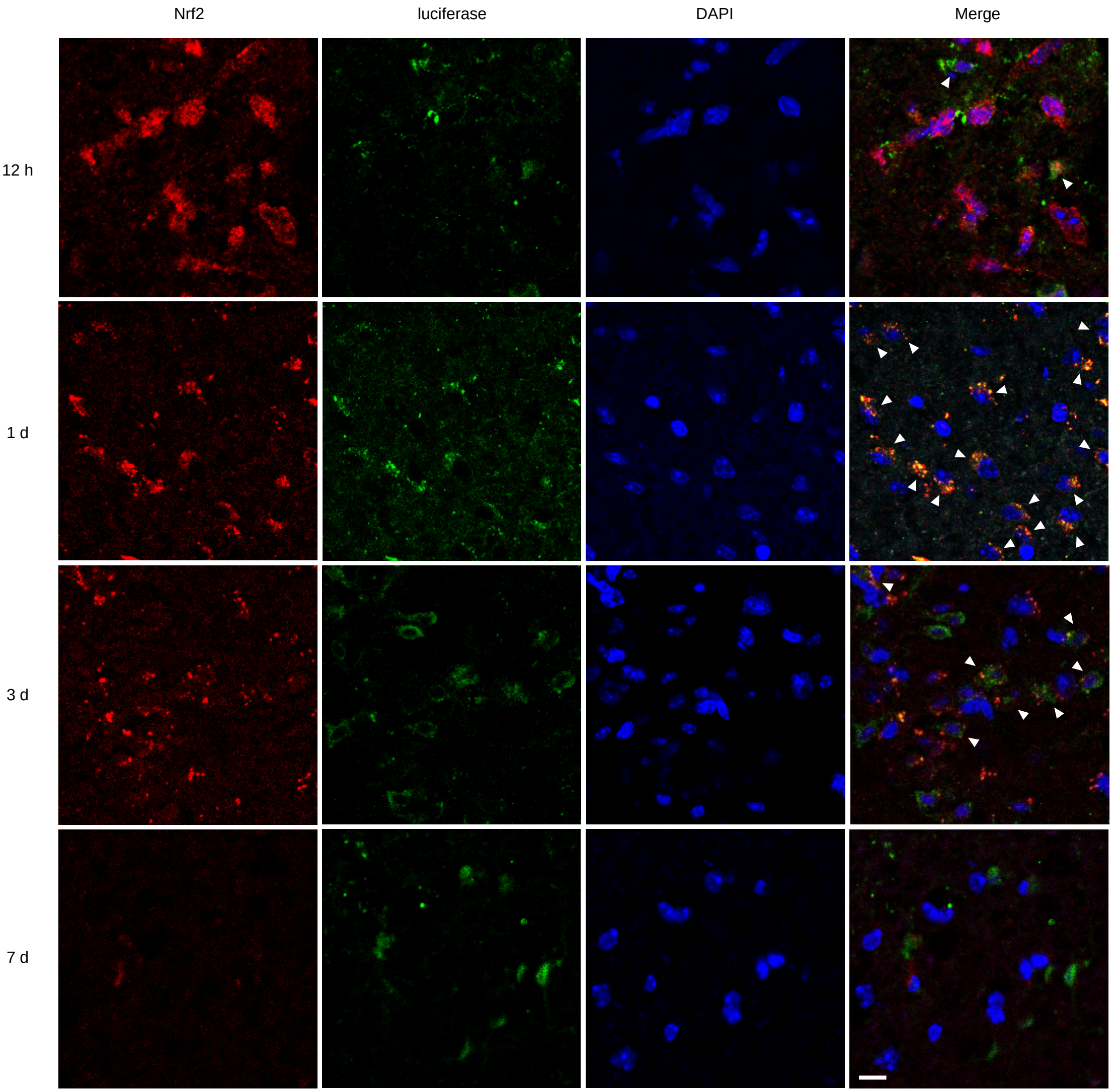

Fig. 4

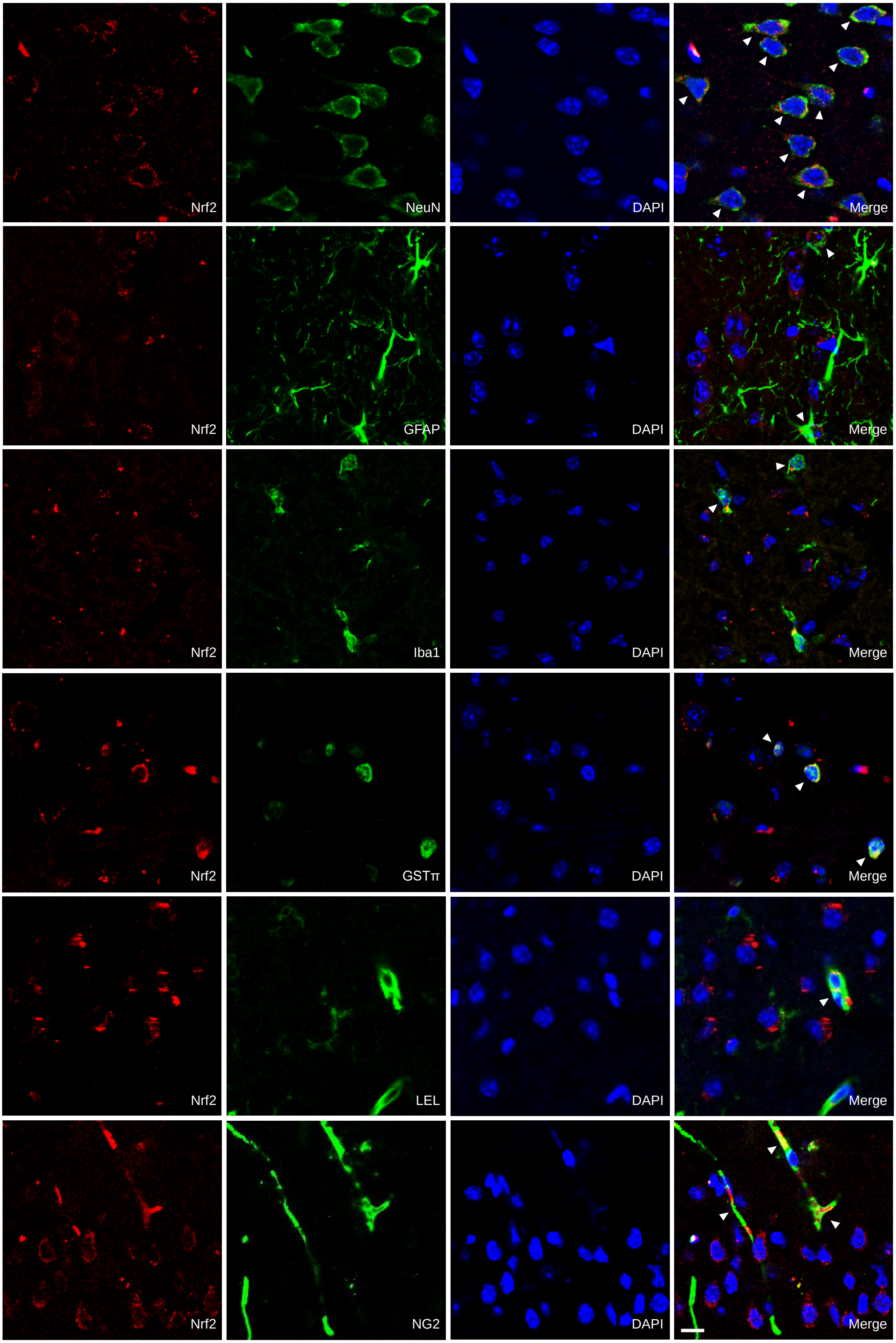
Nrf2
NeuN
DAPI
Merge
Nrf2
GFAP
DAPI
Merge
Nrf2
Iba1
DAPI
Merge
Nrf2
GSTπ
DAPI
Merge
Nrf2
LEL
DAPI
Merge
Nrf2
NG2
DAPI
Merge